JOURNAL OF Materials CHEMISTRY

Delamination and restacking of layered double hydroxides†

Fabrice Leroux,* Mariko Adachi-Pagano, Mourad Intissar, Samuel Chauvière, Claude Forano* and Jean-Pierre Besse

Laboratoire des Matériaux Inorganiques, CNRS UPRES-A no. 6002, Université Blaise Pascal, 63177 Aubière cédex, France. E-mail: forano@cicc.univ-bpclermont.fr; E-mail: fleroux@chimtp.univ-bpclermont.fr

Received 20th April 2000, Accepted 10th July 2000
First published as an Advance Article on the web 6th October 2000

Layered double hydroxides recovered after exfoliation have been characterized by solid state chemistry techniques. The nature of the recovered materials is highly dependant on the drying process; when gently dried, a well-ordered phase is obtained, either by freeze-drying or reconstruction, but the material becomes amorphous after evaporation of the solvent. Delamination was used to prepare interstratified LDHs, making this technique a new route to the formation of a wide range of tunable materials.

Introduction

It is of interest to prepare highly dispersed phases from low-dimensional solids and, to some extent, single layers. Much research has been devoted to this field, which is rapidly expanding to include a large number of materials.[1,2] Exfoliation is of practical use in preparing pillared materials and is also involved in nanocomposite preparation.[3,4] By taking advantage of the anisotropy in the chemical bonding, individual layers may be obtained by spontaneous exfoliation of the solids in aqueous solution. This is the case for clay minerals with lower layer charge density, such as laponite, which readily swells in water.[5,6] More generally, dispersion of clays in water, so-called "liophobic colloidal systems", has been extensively studied with regard to smectite-type materials.[7,8] Added to their relatively low layer charge, these systems display characteristics conducive towards exfoliation, such as an edge to surface net charge difference combined with a small particle size. It is well established that the two properties promote the de-aggregation process, with the former considered as an initiator of exfoliation. Although delamination is much more difficult when the layers are tightly bound together, *i.e.* when the charge density of the layers is high, and where the particle size is large, in order to achieve exfoliation, it is necessary to diminish the attractive forces between layers *via* the exchangeable ions. One method consists of converting the 2D solid into its protonic form and reacting this with a suitable large basic molecule, *e.g.* layered protonic titanate with alkyl ammonium cations.[9,10] Exfoliation is observed after stirring for seven days at room temperature. Exfoliation of zirconium hydrogen phosphate[11] and oxovanadium phosphate[12] requires propyl or butylamine. Delamination of layered chalcogenides was reported for MoS_2[13,14] and TaS_2.[15] MoS_2 disperses into single layers on reaction of Li_xMoS_2 with water, allowing the preparation of a large variety of nanocomposites.[16] In the case of layered double hydroxides, a two-step method has been used to obtain a highly stable colloidal suspension; exchange with an anionic surfactant was followed by reaction in refluent BuOH.[17] In contrast to their cationic counterparts, anionic clays display a layer charge density as high as for mica associated with a large particle, making ultrasonic treatment inefficient in pushing apart the layers. Up to now, the incorporation of large guest compounds such as polyoxometallate anions, such as α-$(SiW_{11}O_{39})^{8-}$,[18] or metalloporphyrin anions[19] into an LDH matrix is only successful after preswelling using spacers, such as terephthalate ions,[20] or by reconstruction.[21] After transformation into an amorphous state (often referred to as the LDO—layered double oxide) *via* thermal treatment, LDH materials can be recovered. However, this process is not universal; some compositions (such as Co_RFe; R is the ratio of M^{II} to M^{III}) do not present such behavior due to the formation of stable phases at high temperature or due to their surface acidity.[21] Alternative methods for exchange reactions with large guest compounds are: direct synthesis by adjusting the pH,[22] reaction in an ethanol–water mixture,[23] or in glycerol,[24] or micellar organic phase extraction.[25]

In this paper, we describe the delamination of the dodecylsulfate-exchanged LDH $Zn_RAl(OH)_{2(1+R)}\{CH_3(CH_2)_{11}SO_4\}\cdot nH_2O$ and its reconstitution. We will show that our method can be used to prepare a wide range of materials, such as those obtained by interstratification of two LDHs with layer charge densities matching each other. Delamination–restacking represents a new pathway for the preparation of tunable materials from LDHs.

Experimental section

Preparation of the materials, and description of the delamination process

The starting materials (Cl)-Zn_RAl ($R=2$, 3 and 4) were prepared by a coprecipitation, as described by Miyata.[26] A solution of $ZnCl_2$ (Aldrich) and $AlCl_3$ (Aldrich) in the molar ratio R was prepared. This solution was added dropwise into 250 ml decarbonated water under vigorous stirring, at a constant pH value depending on R (pH = 8.3, 8.7 and 9.3 for $R=2$, 3, and 4, respectively). The addition of NaOH (1 M) was complete after 24 h. The suspension was aged in the mother liquor with stirring for 24 h. The white solid products were isolated by repeated centrifuging and washing with decarbonated water and were finally dried at room temperature.

The amount of sodium dodecylsulfate salt (Prolabo, 98%) added corresponded to twice the anionic exchange capacity (AEC) of the LDHs. The solution was stirred for 72 h under a nitrogen atmosphere. The exchanged (DS)-LDH was isolated using the same technique described for the pristine material.

†Basis of a presentation given at Materials Discussion No. 3, 26–29 September, 2000, University of Cambridge, UK.

DOI: 10.1039/b002955f

After drying at room temperature, 20 mg of the DS-exchanged LDH was dispersed in 100 ml butanol by a 15 min ultrasonic treatment, and then placed under nitrogen gas. BuOH (Acros, 99%) was used as received. The delamination process was performed overnight under reflux conditions at 120 °C. Larger amounts of surfactant derivative LDH, up to 150 mg, delaminate in 100 ml BuOH solution over a longer period.

Solid materials were recovered after drying. The solvent was removed by evaporation at 120 °C or by freeze-drying. The dried materials were washed with decarbonated water and then dried at room temperature. Restacking of the LDH layers in the presence of Cl^- or CO_3^{2-} ions was performed by adding an aqueous solution containing the sodium salt to the mother liquor. The materials obtained were characterized by elemental analysis (Service Central d'Analyse, CNRS, Vernaison, France).

Characterization techniques

Powder X-ray diffraction patterns were obtained with a Siemens D500 diffractometer (Cu-Kα radiation). Patterns were recorded over the 2θ range 2 to 75° in steps of 0.04° with a count time of 2 s. FTIR spectra were recorded on a Perkin-Elmer 2000 FT spectrometer employing the KBr dilution technique. Thermogravimetric (TG) analysis were performed on a Setaram TGA 92 instrument with a linear heating rate of 5 °C min^{-1} under air. Scanning electron micrographs were recorded with a Cambridge Stereoscan 360 operating at 20 kV at Techinauv, A. S. (Aubière, France).

X-Ray absorption spectroscopy

Zn K-edge XAFS (X-ray absorption fine structure) studies were performed at LURE (Orsay, France) using X-ray synchrotron radiation emitted by the DCI storage ring (1.85 GeV positrons, average intensity of 250 mA) at the D44 line. Data were collected at room temperature in transmission mode at the Zn K-edge (9658.6 eV). The quantity of powdered sample was chosen to obtain edge jumps of about $\Delta\mu x \approx 1$. A double-crystal Si(111) monochromator scanned the energy in 2 eV steps from 100 eV below to 900 eV above the Zn K absorption edge, three spectra were recorded for each sample. The accumulation time was 2 s per point. After extraction by standard procedures, the EXAFS spectra were evaluated by the classical plane wave single scattering approximation. Long metal to metal distance correlations P3 and P4 (see text) arising from multiple scattering phenomena were not refined. Fourier transformations of EXAFS spectra were made after multiplication of the signal by a k^3 factor over a 2.8–14 $Å^{-1}$ Kaiser apodization window with $\tau = 2.5$. The resultant $\chi(k)$ signal was fitted by using the formula $\chi(k) = S_0^2 \Sigma A_i(k) \sin[2kr_i + \phi_i(k)]$ with the amplitude $A_i(k) = (N_i/kr_i^2)F(k) \exp(-2k^2\sigma_i^2)$, where r_i is the interatomic distance, ϕ_i the total phase shift of the ith shell, N_i the effective coordination number, σ_i the Debye–Waller factor, and F_i(k) the backscattering amplitude. EXAFS signal treatments[27] and refinements were performed using a proprietary program package at LURE.[28] The residual ρ factor is defined as $\rho = [\Sigma\{k^3\chi_{exp}(k) - k^3\chi_{theo}(k)\}^2/\Sigma\{k^3\chi_{exp}(k)\}^2]^{1/2}$. To estimate the relative part of the cations contributing to the metal–metal correlation, the number of backscattering atoms was free to move during the refinement. This guarantees all possible ratios between Al^{3+} and Zn^{2+} for the second shell. The commonly accepted fitting accuracy is about 0.02 Å for the distance and 10 to 20% for the number of neighbors.

Table 1 Chemical analysis of (Cl)-Zn_2Al and its DS derivative

Sample	Chemical Formulae
(Cl)-Zn_2Al[a]	$[Zn_{0.67}Al_{0.33}(OH)_2]Cl_{0.33}\cdot 1.07H_2O$
(DS)-Zn_2Al	$[Zn_{0.67}Al_{0.33}(OH)_2]\{CH_3(CH_2)_{11}SO_4\}_{0.32}\cdot 2.1H_2O$

[a]Molecular mass of 117.7, leading to an AEC of 2.80 meq g^{-1}.

Results and discussion

Characterization of Zn_RAl LDHs

The molar ratio Zn/Al and the relative ion contents of the prepared materials are very close to the expected values, indicating that the reaction was complete (Table 1). As the Zn_2Al sample shows the highest layer charge in the LDH series, the delamination process was studied in detail.

Zn_RAl materials are well crystallized, as can be seen from the X-ray diffraction pattern (Fig. 1), the diffraction peaks are typical of the layered double hydroxide structure.[29] The reflections were indexed in a hexagonal lattice with a $R\bar{3}m$ rhombohedral symmetry, commonly used as a description of the LDH structure. Miller indexing is given in Fig. 1 and refined cell parameters are reported in Fig. 2. An increase in the Zn to Al ratio increases the unit cell parameters. As a corresponds to the metal to metal distance, replacement of Zn^{2+} cations by the smaller Al^{3+} cations

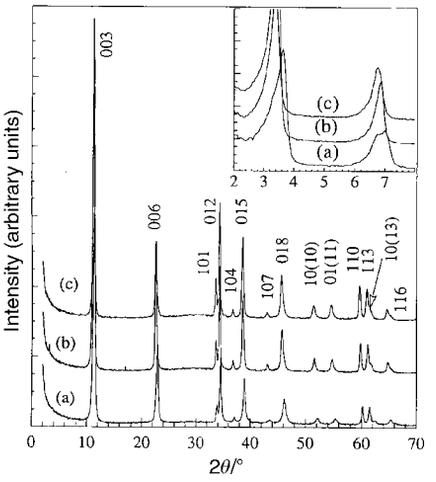

Fig. 1 Diffraction patterns of (Cl)-Zn_RAl, (a) $R=2$, (b) $R=3$ and (c) $R=4$. The first two reflections of the DS derivative are displayed in the inset.

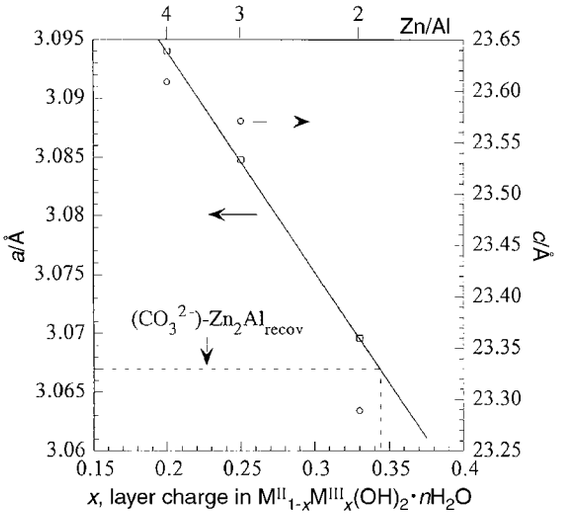

Fig. 2 Evolution of the lattice parameters a (square) and c (circle) as a function of R. The layer charges of (CO_3^{2-})-Zn_2Al_{recov} was estimated from the (110) position (see text).

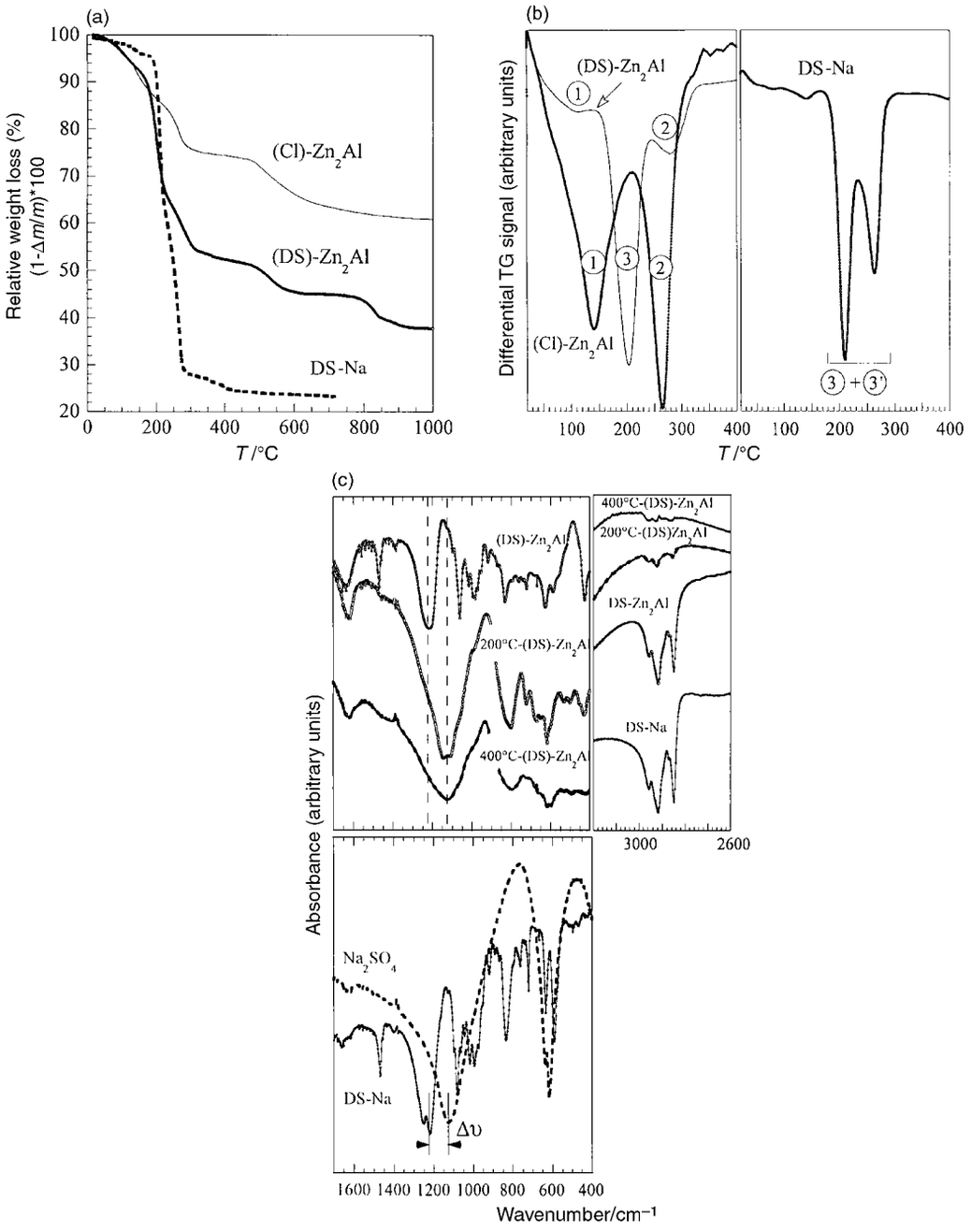

Fig. 3 DTA and DTG diagrams of (Cl)-ZnAl, (DS)-ZnAl and DS: (a) DTA and (b) DTG (weight losses are indicated). (c) FTIR spectroscopy: IR spectra of the sample heated to 200 and 400 °C and of Na_2SO_4 are also shown.

in the octahedral sheet decreases the *a* parameter. The increase in the interlamellar distance is related to the decrease of the net charge of the layers with the gradually diminishing Al^{3+} content as the cause of the expansion of the layers.

DS incorporation between the layers of the Zn_RAl LDHs phases is confirmed by the increase in the basal spacing. Its value is the sum of the layer thickness, estimated to be 4.8 Å for the brucitic-like layers, and the interlayer distance. A basal spacing of 25.2 Å (Fig. 1 inset) indicates that the surfactant tails are interdigitated in the interlamellar space, as the length of the whole DS molecule is 20.8 Å.[30] Our attempts to prepare ZnAl LDHs with the same DS arrangment (bilayer) as in Ni_4Al[31] and Mg_2Al LDH[32] were not successful.

The thermal behaviour of DS-exchanged derivatives was studied (Fig. 3a). To assign weight losses, thermogravimetric analysis was also conducted on sodium dodecylsulfate salt. DS-Na decomposes in two steps, centered at 210 (denoted 3) and 255 °C (denoted 3′). The total weight loss is in agreement with the formation of sodium sulfate (observed by X-ray diffraction at 700 °C) from two surfactant molecules ($\Delta m_{exp} = 76.5\%$, $\Delta m_{th} = 75.4\%$). The small DTA signal (Fig. 3b) before 100 °C indicates a conformational rearrangment of the molecule before it decomposes. For (Cl)-Zn_2Al, loss of intracrystalline water (1) and dehydroxylation (2) occurs at 150 and 250 °C, respectively. For the DS derivative, the three processes (1 + 2 + 3) below 400 °C are superimposed (Fig. 3b), making it difficult to dissociate the water loss and dehydroxylation (1 + 2) processes from the decomposition of the organic species. Due to intercalation, decomposition of interlayer DS does not proceed as described for the surfactant molecule. Decomposition of the alkyl chains is the first process. The CH_2 vibration bands disappear in the IR spectra of (DS)-Zn_2Al heated to 200 °C, and are completely absent after 400 °C (Fig. 3c). In the meantime, the SO_4 polyhedra

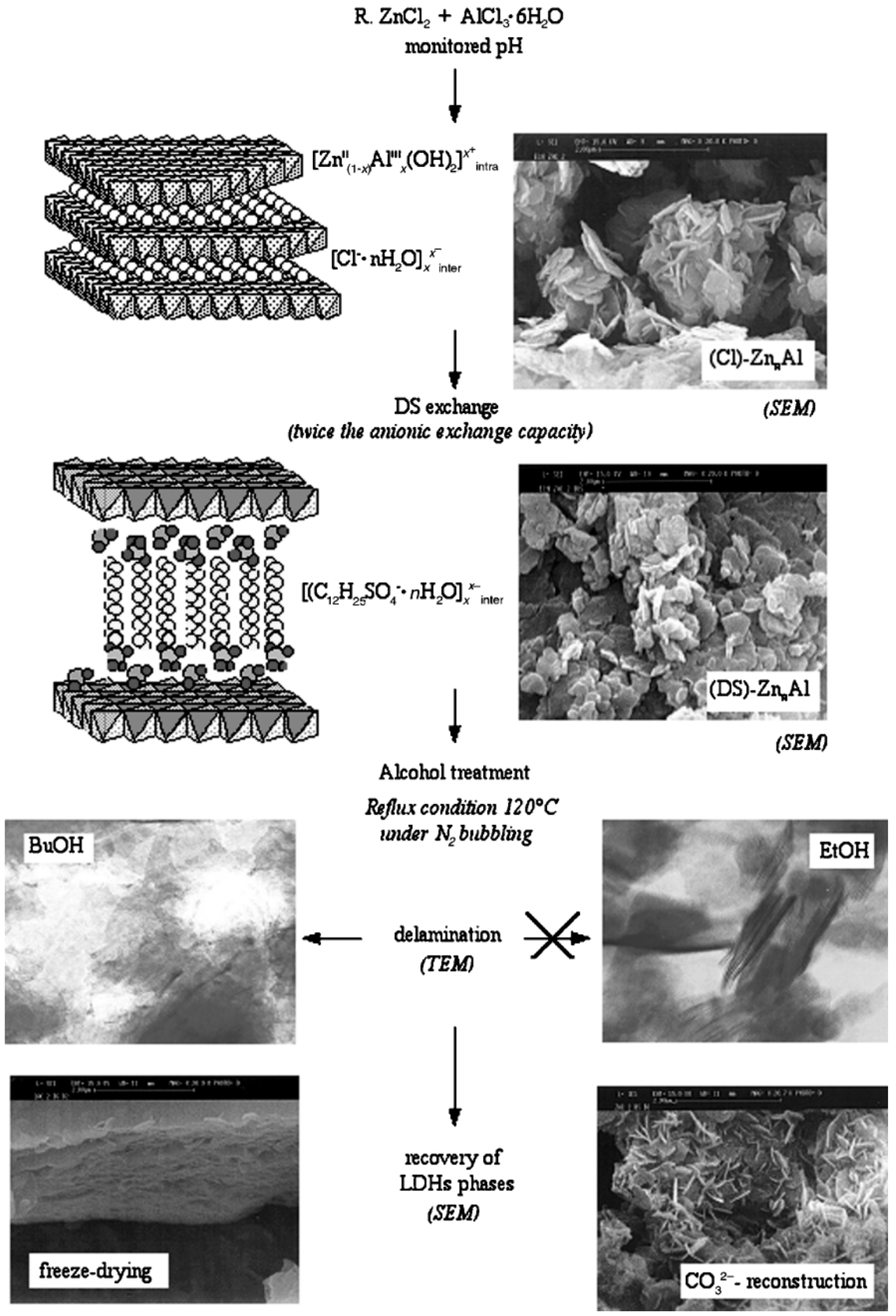

Fig. 4 Pathways for LDH synthesis, DS-exchange, delamination in BuOH and recovery by drying. The morphology of the samples is indicated by SEM or TEM pictures.

vibration is shifted by *ca.* 100 cm^{-1} to lower frequency, indicating the local symmetry changes from $C3v$ (in DS) to T_d in SO_4^{2-} (Fig. 3c). This entire thermal process has been proposed previously.[31]

As Zn^{2+} and Al^{3+} retain the same oxidation state during the thermal treatment, the molecular mass can be calculated from the total weight loss according to the equation: M_W of $Zn_RAl(OH)_{2(1+R)}\{CH_3(CH_2)_{11}SO_4\}\cdot nH_2O^*(1-\Delta m/m) = M_W$ of "$Zn_RAlO_{R+3/2}$", where $\Delta m/m$ represents the weight loss in percent obtained from the TGA curve (Fig. 3a). M_w obtained

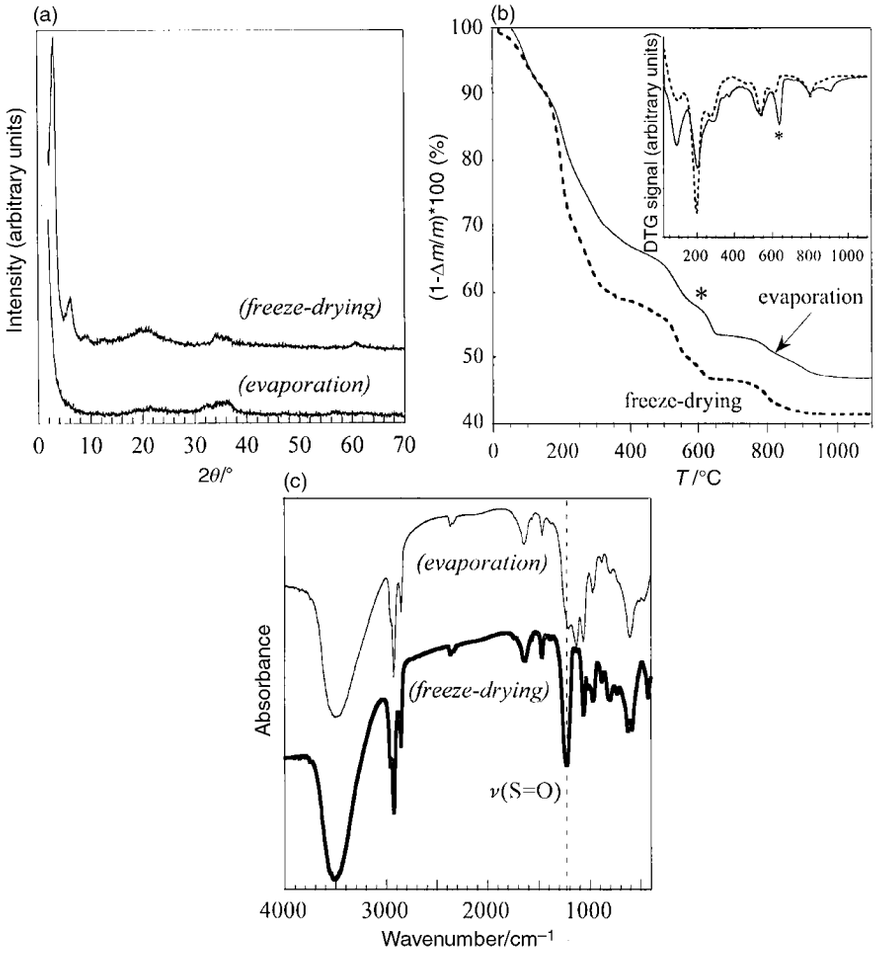

Fig. 5 Comparison of recovered materials after freeze-drying and evaporation: (a) X-ray diffraction, (b) thermal analysis and (c) FTIR spectroscopy.

from this equation is in agreement with the elemental analysis data [for $R=2$, $\Delta m/m=0.63$ ($\Delta m/m_{\text{theor}}=0.66$); for $R=3$, $\Delta m/m=0.58$ ($\Delta m/m_{\text{theor}}=0.58$)].

Delamination process

The process of delamination in BuOH is summarized in Fig. 4. Other solvents were also used. It was previously mentioned that dispersion of (DS)-Zn_2Al in methanol, ethanol, propanol or hexane under reflux conditions yields unstable colloidal suspensions, whereas higher alcohols, such as pentanol and hexanol, give rise to stable translucent solutions. The optimal time for completion of the delamination process depends on the nature of the LDH material. Twelve hours reaction was required for complete delamination of Zn_2Al.

Before any treatment, the samples were dried at room temperature. It is well known that the water content has an important effect on the particle texture.[33] Since the water content may also influence the delamination process (*vide infra*), (DS)-Zn_2Al was dried in vacuum overnight. This treatment did not change the X-ray diffraction pattern of the material. After refluxing in BuOH, the resulting solution was cloudy/milky, indicating that the solid was mostly highly dispersed but had not been exfoliated. After one hour, a white powder settled to the bottom of the vessel and this material was dried and analyzed. The phase exhibits a strong contraction of the interlayered domain from 25.2 to 16.8 Å. This indicates a high degree of interdigitation of the alkyl chains. Considering the thickness of the brucitic layer (*vide supra*), the surfactant tails are tilted at *ca.* 57° from the perpendicular axis of the inorganic layers (along *c*). Also, some of the surfactant anions were removed from the interlayer space as indicated by the TG analysis (not shown). The final weight loss step, attributed to the decomposition of SO_4 to SO_2, remained quantitatively high, showing that SO_4^{2-} anions remained in the structure, balancing the layer charge.

Thus, it appears that vacuum treatment impedes delamination of Zn_2Al. The water content plays a major role in the delamination process and we believe that the replacement of the water molecules by the solvent molecules is the key process in exfoliation. The intercrystalline water could also influence the delamination process. Several LDH samples were kept for three to four weeks at various humidities (20, 40, 60 and 80% R.H.). Comparatively, LDHs kept at low RH did exfoliate, although at an R.H. as high as 80% a cloudy BuOH suspension remained. In order to prevent particle aggregation due to the effect of water, freshly prepared (DS)-LDH materials were washed with ethanol, then butanol and directly suspended in BuOH for delamination. The material exfoliated, as was evidenced by the formation of a translucent solution.

Reconstruction

Highly 2D-oriented material was recovered after freeze-drying (Fig. 4) and the X-ray diffraction pattern obtained is displayed in Fig. 5a. Initially, it cannot be said for certain that the recovered solids are LDH-like materials, rather just lamellar materials. No diffraction peak was observed for the sample recovered by evaporation. The interlamellar distance of the freeze-dried material, 29.3 Å, was larger than that of the pristine DS derivative. This may indicate a rearrangment of the DS molecules or the incorporation of further guest molecules into the interlayer space. An additional weight loss is observed at 600 °C for both samples, which is more pronounced after

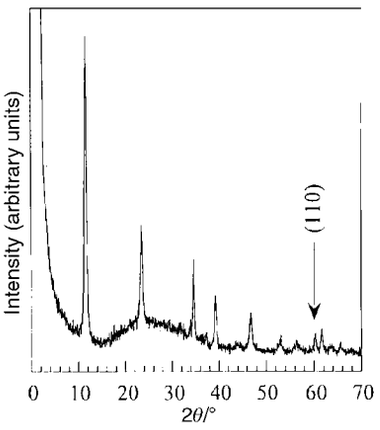

Fig. 6 X-Ray diffraction pattern of the recovered Zn_2Al sample after addition of an aqueous solution of K_2CO_3.

evaporation (Fig. 5b). The SO_4 vibration band was much larger in the latter case, showing that the DS heads are not the sole cause of this peak (Fig. 5c). In all probability, this is related to sulfate groups produced by decomposition of DS. Vibration bands from the inorganic lattice between 400 and 700 cm^{-1} were unchanged compared to the precusor.[34] The general features of the spectra are mostly unchanged after the freeze-drying process, although bands attributed to (O–M) vibrations were broadened after evaporation, due to the loss of stacking cohesion. This shows that the recovered solids are highly sensitive to the drying process, giving either ordered or disordered phases at an atomic scale, as confirmed by XAS studies (*vide infra*).

To test the LDH nature of the solids obtained by BuOH treatment, the samples were reacted with an aqueous K_2CO_3 solution. The Zn/Al ratio was slightly decreased after the delamination–restacking process (Zn/Al_{recov} of 1.94 and 2.81, initial 2.01 and 2.98). The X-ray diffraction pattern of the product exhibits well-defined peaks (Fig. 6), which are characteristics of the LDH structure. The unit cell parameter a can be employed as an appropriate estimation of the metal ratio.[35] The cell parameter a exhibits a linear correlation with the Zn/Al ratio. The position of the (110) peak of the (CO_3^{2-})-Zn_2Al_{recov} material corresponds to a layer charge of 0.345 per metal atom, leading to a Zn/Al ratio of approximately 1.9, close to the value found by chemical analysis. The same trend was found for the (CO_3^{2-})-Zn_3Al_{recov} sample. These results show that refluxing in BuOH induces a slight dissolution of the layers.

Local order study

In order to get a better insight into the delamination process, Zn K-edge spectra were analyzed. The moduli of the Fourier transformations, which correspond to the pseudo-radial distribution function (pseudo-RDF), of the EXAFS spectra of pristine (Cl)-ZnAl and its DS derivatives (with 16 and 25 Å basal spacing) are presented in Fig. 7a. The identical distribution curves show that the local order around the Zn atoms remains unchanged after the intercalation of surfactant anions in both the 16 and 25 Å phases. Furthermore, the long range order is also identical for these two samples, as exemplified by the presence of P3 and P4 peaks, arising from Zn–Me at distances of $\sqrt{3}a$ and $2a$, respectively.[36] As the cations differ in their "electronic weight" (difference in backscattering phase and amplitude functions), the nature of the backscattering atoms composing the second shell of coordination can be distinguished. The refinements of the first two shells, which contain only single scattering contributions, are reported in Table 2. The results for the two samples (16 and 25 Å) are fairly similar, given to the identical distribution functions. The first

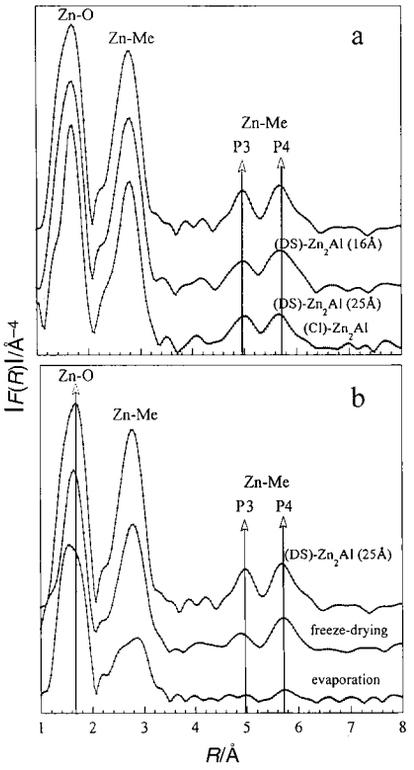

Fig. 7 Fourier transform spectra (Zn K-edge): (a) (Cl)-Zn_2Al, 25 Å-(DS)-Zn_2Al, 16 Å-(DS)-Zn_2Al, (b) delaminated pristine 25 Å-(DS)-Zn_2Al, and the solids recovered by freeze-drying or by evaporation at 120 °C. Distances are given without phase shift corrections.

shell corresponds to the presence of oxygen atoms, the result is in agreement with an octahedral environment of OH groups around the Zn^{2+}. The Zn–O distance is expected to have a value of 2.11 Å in an O_h environment, from bond-valence calculations.[37] The second shell is related to the presence of metal, *i.e.* Al^{3+} and Zn^{2+} cations. For a composition Zn_2Al, intraplanar cationic order comprises a shell around M^{II} composed of 3 Al^{3+} and 3 Zn^{2+} cations, whereas 6 Zn^{2+} ions surround the M^{III} centers.[38,39] The results are close to the idealized sharing of *ca.* 50% between the two cations in the second shell around Zn^{2+}. The total number of cations was slightly overestimated by the $k\chi(k)$ refinement, but the number of neighboring atoms was accurate, within the error limits.

The effect of the delamination process is shown in Fig. 7b by a comparison of the moduli of the Fourier transform spectra of the solids reconstituted by evaporation of the solvent or freeze-drying. At a first glance, the Zn K-edge spectra appear to be

Table 2 Results of the EXAFS fitting procedures. N_i is the coordination number, R_i the distance, σ_i the Debye–Waller factor, and ρ the residual factor

Sample	Bond	N_i	R_i/Å	σ_i^2/Å^2	ρ (%)
(Cl)-ZnAl	Zn–O	6.0	2.09	0.0086	0.4
	Zn–Zn	4.2	3.12	0.0144	
	Zn–Al	4.0	3.00	0.0174	
25 Å-(DS)-ZnAl	Zn–O	5.8	2.08	0.0076	0.5
	Zn–Zn	5.0	3.10	0.0119	
	Zn–Al	4.0	2.99	0.0130	
16 Å-(DS)-ZnAl	Zn–O	6.0	2.08	0.0079	0.6
	Zn–Zn	4.0	3.11	0.0119	
	Zn–Al	3.5	3.01	0.0119	
(DS)-$ZnAl_{recov}$ (freeze-dried)	Zn–O	5.7	2.05	0.0085	0.5
	Zn–Zn	3.0	3.11	0.0117	
	Zn–Al	2.9	3.01	0.0134	
(DS)-$ZnAl_{recov}$ (evaporation)	Zn–O	5.6	2.03	0.0100	0.3
	Zn–Zn	2.5	3.11	0.0161	
	Zn–Al	2.4	3.01	0.0139	

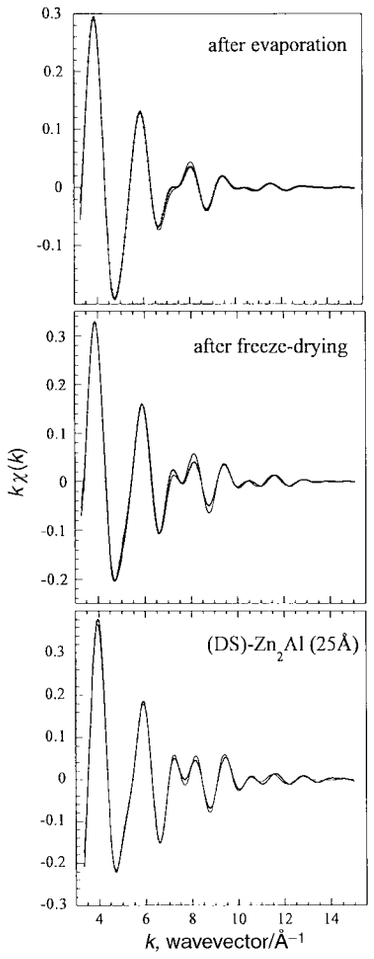

Fig. 8 $k\chi(k)$ Refinement of the first three shells for 25 Å-(DS)-Zn_2Al, and the solids recovered by freeze-drying or evaporation at 120 °C. Dots are experimental data.

similar, retaining most of the expected features for both samples, that is to say Zn–O and Zn–metal correlations. However, the intensity of the P3 and P4 peaks is much reduced (or even absent) for the solid recovered after evaporation. This suggests a random disorder or a strong distortion of the framework, both of which would cancel out the focussing effect which is enhanced by the linear Me–Me situation.[40] Given the data obtained from IR spectroscopy and X-ray diffraction, the first case has to be considered; the material is highly disordered and decomposed, and appears almost amorphous. Zn^{2+} seems to retain a six-fold coordination sphere of oxygen atoms, although the Zn–O distance is shortened from 2.09 to 2.03 Å. Refinement curves are presented in Fig. 8. The recovered samples display a proportion of Zn^{2+} and Al^{3+} cations in the second coordination shell of roughly 50% each. In spite of its amorphous nature, the material recovered after evaporation shows the atomic arrangment characteristic of the local order of Zn_2Al LDH, ruling out the possibility of phase segregation.

Delamination was used to synthesize composite LDH materials by interstratification during recovery. Nanocomposites with alternating layers have previously been prepared by reaction of MoS_2 single layers with Co^{2+}[41] or intercalation of $LiAl_2(OH)_6^+$ into montmorillonite.[42] Some minerals, such as tochilinite[43] or yushikinite,[44] also present alternating layers; in these two cases, MgAl LDH-like layers alternate with incommensurable layers of Fe_xS or VS_2, respectively. LDH materials were chosen so that their layer charge densities matched (same M^{II}/M^{III} ratio). Solutions of delaminated (DS)-Zn_2Al and (DS)-Zn_2Cr were mixed, BuOH treatment was carried out for an additional 12 h and the solution was allowed

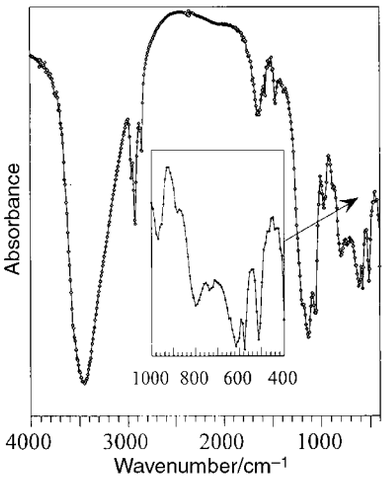

Fig. 9 FTIR spectrum of an interstratified LDH of average layer composition "$(Zn_2Al)_{1-p}(Zn_2Cr)_p(OH)_2$".

to evaporate at 120 °C. The solid obtained remained amorphous. Several lattice vibrations are clearly visible in the IR spectrum of the product (Fig. 9). The general cation composition can be written as $(Zn_2Cr)_p(Zn_2Al)_{1-p}$ ($p \approx 0.5$). The characterization of this composite material and interstratification of other LDHs are presently being studied.

Conclusion

The dodecylsulfate of Zn_2Al LDH was exfoliated in BuOH solution. The delamination process was sensitive to the preparation mode, and especially the drying process. We also succeeded in delaminating (DS)-Zn_RAl materials.

After recovery, the ratio of surfactant to LDH was found to be altered, particularly after evaporation of BuOH at 120 °C, leading to an amorphous-like material. However, small structural units are visible by X-ray absorption spectroscopy.

Acknowledgements

The authors are grateful to Dr V. Briois for her assistance with the XAS experiments and to Dr H. Roussel for having compared the XAS refinements using FeFF6. We acknowledge the experimental opportunities at LURE (Orsay, France).

References

1 J. Jacobson, in *Comprehensive Supramolecular Chemistry: Colloidal Dispersion of Compounds with Layer and Chain Structures*, ed. G. Alberti and T. Bein, Elsevier, Oxford, 1996, vol. 7, p. 315.
2 R. Schöllhorn, *Chem. Mater.*, 1996, **8**, 1747.
3 P. B. Messersmith and E. P. Giannelis, *Chem. Mater.*, 1994, **6**, 1719.
4 Z. Wang and T. J. Pinnavaia, *Chem. Mater.*, 1998, **10**, 3769.
5 J. D. F. Ramsay, *J. Colloid. Interface Sci.*, 1986, **109**, 441.
6 P. A. Brahimi, P. Labbe and G. Reverdy, *Langmuir*, 1992, **8**, 1908.
7 S. Sonin, *J. Mater. Chem.*, 1998, **8**, 2557.
8 H. van Olphen, in *Chemistry of Clays and Clay Minerals*, ed. A. C. Newman, Wiley, New York, 1987, p. 203.
9 T. Sasaki and M. Watanabe, *J. Am. Chem. Soc.*, 1998, **120**, 4682.
10 H. Rebbah, M. M. Borel and B. Raveau, *Mater. Res. Bull.*, 1980, **15**, 317.
11 E. W. Stein, Sr., C. Bhardwaj, C. Y. Ortiz-Avila, A. Clearfield and M. A. Subramanian, *Mater. Sci. Forum*, 1994, **115**, 152.
12 T. Nakato, Y. Furumi, N. Terao and T. Okuhara, *J. Mater. Chem.*, 2000, **10**, 737.
13 P. Joensen, E. D. Crozier, N. Alberding and R. F. Frindt, *J. Phys. C: Solid State Phys.*, 1987, **20**, 4043.
14 J. Heising and M. G. Kanatzidis, *J. Am. Chem. Soc.*, 1999, **121**, 638.
15 L. F. Nazar and A. J. Jacobson, *J. Mater. Chem.*, 1994, **4**, 1419.
16 M. G. Kanatzidis, R. Bissessur, D. C. de Groot, J. L. Schindler

and C. R. Kannewurf, *Chem. Mater.*, 1993, **5**, 595, and references therein.
17 M. Adachi-Pagano, C. Forano and J.-P. Besse, *Chem. Commun.*, 2000, 91.
18 E. Narita, P. D. Kaviratna and T. J. Pinnavaia, *J. Chem. Soc., Chem. Commun.*, 1993, 60.
19 S. Bonnet, C. Forano, A. de Roy, J.-P. Besse, P. Maillard and M. Momenteau, *Chem. Mater.*, 1996, **8**, 1962.
20 M. A. Drezdon, *Inorg. Chem.*, 1988, **27**, 4628.
21 K. Chibwe and W. Jones, *J. Chem. Soc., Chem. Commun.*, 1989, 926.
22 F. Kooli and W. Jones, *Inorg. Chem.*, 1995, **34**, 6238.
23 T. Hibino and A. Tsunashima, *Chem. Mater.*, 1997, **9**, 2082.
24 E. D. Dimotakis and T. J. Pinnavaia, *Inorg. Chem.*, 1990, **29**, 2394.
25 E. L. Crepaldi, P. C. Pavan and J. B. Valim, *Chem. Commun.*, 1999, 155.
26 S. Miyata, *Clays Clay Miner.*, 1983, **31**, 305.
27 G. McKale, B. W. Veal, A. P. Paulikas, S.-K. Chan and J. Knapp, *J. Am. Chem. Soc.*, 1988, **110**, 3763.
28 A. Michalowicz, Round Midnight, EXAFS Signal Treatment and Refinement Programs, LURE, Orsay, France. Programs available on the LURE Web site; http://www.LURE.fr.
29 M. Bellotto, B. Rebours, O. Clause, J. Lynch, D. Bazin and E. Elkaïm, *J. Phys. Chem.*, 1996, **100**, 8527.
30 S. Sundell, *Acta Chem. Scand. A*, 1971, **31**, 799.
31 A. Clearfield, M. Kieke, J. Kwan, J. L. Colon and R.-C. Wang, *J. Inclusion Phenom. Mol. Recognit. Chem.*, 1991, **11**, 361.
32 T. Kanoh, T. Shichi and K. Takagi, *Chem. Lett.*, 1999, 117.
33 S. K. Yun and T. J. Pinnavaia, *Chem. Mater.*, 1995, **7**, 348.
34 J. T. Kloprogge and R. L. Frost, *J. Solid State Chem.*, 1999, **146**, 506.
35 E. Lopez-Salinas, M. Garcia-Sanchez, J. A. Montoya, D. R. Acosta, J. A. Abasolo and I. Schifter, *Langmuir*, 1997, **13**, 4748.
36 H. Roussel, V. Briois, E. Elkaïm, A. de Roy and J.-P. Besse, *J. Phys. Chem.*, 2000, **104**, 5915.
37 N. E. Brese and M. O'Keefe, *Acta Crystallogr., Sect. B*, 1991, **47**, 192.
38 W. Hofmeister and H. von Platen, *Cryst. Rev.*, 1992, **3**, 3.
39 M. Vucelic, W. Jones and G. D. Moggridge, *Clay Clay Miner.*, 1997, **45**, 803.
40 N. Alberding and E. D. Crozier, *Phys. Rev. B*, 1983, **27**, 3374.
41 S. Golub, C. Payen, G. A. Protzenko, Yu. N. Novikov and M. Danot, *Solid State Commun.*, 1997, **102**, 419.
42 Q. Feng, C. Honbu, K. Yanagisawa, N. Yamasaki and S. Komarneni, *J. Mater. Chem.*, 2000, **10**, 483.
43 G. A. Kakos, T. W. Turney and T. B. Williams, *J. Solid State Chem.*, 1994, **108**, 102.
44 Y. Moëlo, O. Rouer, L. Cario and B. Cervelle, *Miner. Mag.*, 1999, **63**, 879.